The effect of impurities on the piezoelectric properties of lithium germanate

1979 J. Phys. D: Appl. Phys. 12 611

(http://iopscience.iop.org/0022-3727/12/4/018)

J. Phys. D: Appl. Phys., Vol. 12, 1979. Printed in Great Britain

The effect of impurities on the piezoelectric properties of lithium germanate

D S Robertson†, I M Young†, F W Ainger‡, C O'Hara‡ and A M Glazer§
† Royal Signals and Radar Establishment, St Andrews Road, Great Malvern, Worcs
‡ Plessey Research Limited, Allen Clark Research Centre, Caswell, Towcester, Northants
§ Clarendon Laboratory, University of Oxford, Parks Road, Oxford

Received 23 October 1978

Abstract. Crystals of lithium germanate (Li_2GeO_3) and of Li_2GeO_3 containing small amounts of silicon and magnesium were grown by the Czochralski method. The elastic, piezoelectric and dielectric tensor components were measured over the temperature range -40 to $+100$°C. Crystal quality deteriorated drastically at SiO_2 contents (in the melt) greater than 2 wt % and at MgO contents greater than 1 wt %. There was some degradation in piezoelectric properties at impurity levels giving tolerable crystal quality. The evaluation of the crystals with regard to surface acoustic wave applications is discussed.

1. Introduction

The technique of controlling the properties of crystals by adding impurities in a controlled manner is well established. For example, the optical properties of lithium niobate have been altered by the addition of magnesium oxide (Dridenbaugh *et al* 1970), and the pyroelectric properties of triglycine sulphate and lead germanate have been altered by the addition of alanine and barium respectively (Lock 1971, Watton *et al* 1976). It was considered of possible practical importance to make impurity additions to a piezoelectric crystal and examine their effect on the piezoelectric properties. The crystal chosen for these studies was lithium germanate, which has been shown to be piezoelectric but not ferroelectric (Ainger *et al* 1971). The lattice of the lithium germanate structure is orthorhombic and the space group symmetry is $Cmc2_1$ belonging to point group *mm2* (Vollenkle and Wittmann 1968).

2. Experimental details

2.1. Crystal growth

The crystals were grown by the Czochralski technique using a growth rate of 3 mm h^{-1} and a rotation rate of 10 rpm. The melt for the pure crystals was prepared from stoichiometric quantities of high-purity lithium carbonate and germanium dioxide, and the melting temperature was 1200 °C. Air was passed through the growth chamber at a rate

0022-3727/79/040611+08 $01.00

of 500 ml min^{-1}. Initially the obvious substitutions appeared to be the partial substitution of lithium by other group 1A elements, e.g. sodium, and the partial substitution of germanium by other group 4B elements, e.g. silicon. In the event the former were not attempted since all the other group 1A germanates are very hygroscopic. Lithium germanate is itself hygroscopic and there seemed little value in increasing this tendency. Partial substitution of lithium by magnesium was attempted since magnesium has the smallest ion size in group 2A after the toxic element beryllium. Substitutions for germanium were confined to silicon. The substituent elements were added as oxides to melts of pure lithium germanate.

2.2. Measurements

The following bulk properties were measured: the tensor components of the elasto-piezo-dielectric matrix (figure 1), the thermal expansion coefficients in the three principal crystallographic directions, and the pyroelectric coefficient. Elastic moduli were determined over the temperature range -40 to $+100\,°C$.

S_{11}^E	S_{12}^E	S_{13}^E	0	0	0	0	0	d_{31}
S_{12}^E	S_{22}^E	S_{23}^E	0	0	0	0	0	d_{32}
S_{13}^E	S_{23}^E	S_{33}^E	0	0	0	0	0	d_{33}
0	0	0	S_{44}^E	0	0	0	d_{24}	0
0	0	0	0	S_{55}^E	0	d_{15}	0	0
0	0	0	0	0	S_{66}^E	0	0	0
0	0	0	0	d_{15}	0	ϵ_{11}^T	0	0
0	0	0	d_{24}	0	0	0	ϵ_{22}^T	0
d_{31}	d_{32}	d_{33}	0	0	0	0	0	ϵ_{33}^T

Figure 1. Elasto-piezo-dielectric matrix for Li_2GeO_3 (class *mm*2).

The elastic and piezoelectric coefficients were determined from resonant and antiresonant frequency measurements on suitably oriented bars and plates, following the procedure described in the *IRE Standards* (1958). The specimen shapes and orientations were the same as those used by Namamatsu *et al* (1973) for lithium gallate. The dimensions were typically 8 mm × 2 mm × 1 mm for the bars and 5 mm × 5 mm × 1 mm for the

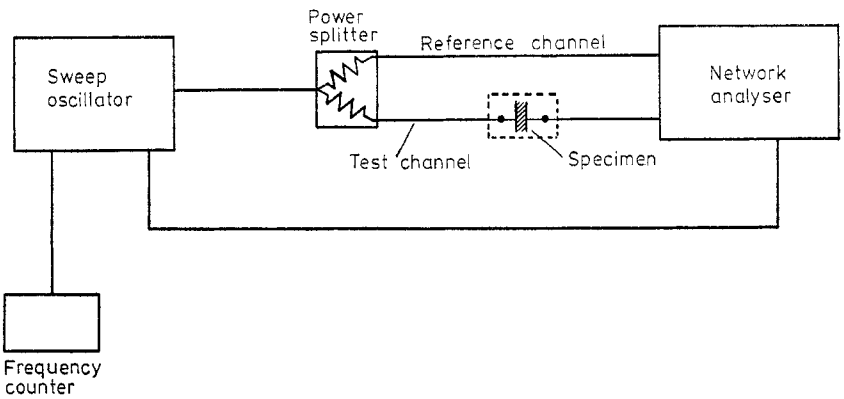

Figure 2. Circuit for measurement of resonant and antiresonant frequencies.

Table 1. Effective elastic and piezoelectric coefficients for the different specimens.

Specimen	$\bar{S}$ (or $\bar{C}$), d, $\bar{k}$
(1) (*zxtwl*) bar	S_{31}^{E}, d_{31}, k_{31}
(2) (*zytwl*)0°/0°/0° bar	S_{32}^{E}, d_{32}, k_{32}
(3) (*yztwl*)0°/0°/0° bar	S_{33}^{E}, d_{33}, k_{33}
(4) (*xytwl*)0°/0°/0° square plate	$C_{55}^{E}/(1-k_{15}^{2})$, k_{15}
(5) (*yxtwl*)0°/0°/0° square plate	$C_{44}^{E}/(1-k_{24}^{2})$, k_{24}
(6) (*xztwl*)0°/30°/0° bar	$\frac{1}{16}(S_{11}^{E}+6S_{13}^{E}+9S_{33}^{E}+3S_{55}^{E})$ $\frac{1}{8}(-3d_{15}+d_{31}+3d_{33})$
(7) (*yztwl*)0°/−45°/0° bar	$\frac{1}{4}(S_{22}^{E}+2S_{23}^{E}+S_{33}^{E}+S_{44}^{E})$ $\frac{1}{2\sqrt{2}}(-d_{24}+d_{32}+d_{33})$
(8) (*xztwl*)0°/45°/0° square plate	$\frac{1}{2}(C_{44}^{E}+C_{66}^{E})$
(9) (*zxtwl*)−30°/0°/0° bar	$\frac{1}{16}(9S_{11}^{E}+6S_{12}^{E}+S_{22}^{E}+3S_{66}^{E})$ $\frac{1}{4}(3d_{31}+d_{32})$
$S_{44}=1/C_{44}$, $S_{55}=1/C_{55}$, $S_{66}=1/C_{66}$	

plates. Specimens were electroded by vacuum-depositing 0·5–0·6 μm of gold (on top of about 300 Å of chromium) on to the appropriate faces and attaching short lengths (about 10 mm) of 0·1 mm diameter copper wire, using a silver-loaded epoxy resin (Emerson and Cuming Eccobond 56c). The latter was applied sparingly in order to minimise the mass loading. Resonant and antiresonant frequencies (f_r, f_a) were determined from transmission measurements using a Hewlett Packard network analyser system comprising a sweep oscillator type 8601A, network analyser 8407A and display unit 8412A. The circuit is shown in figure 2. To permit measurements at different temperatures the specimens were housed in a Montford Mini-K environmental test chamber operating over the range −40 to +100 °C.

Table 1 lists the specimen orientations and shapes, the effective elastic and piezoelectric coefficients and the effective electromechanical coupling factors. The effective coefficients were obtained directly from the measured f_r and f_a values using the following formulae:

For bars 1, 2, 6, 7 and 9

$$\bar{S}=\frac{1}{4\rho l^2 f_r^2}$$

$$\frac{\bar{k}^2}{\bar{k}^2-1}=\frac{\pi f_a}{2 f_r}\cot\left(\frac{\pi f_a}{2 f_r}\right)$$

$$\bar{d}=\bar{k}(\bar{S}\bar{\epsilon})^{1/2}$$

where ρ is the density and l the length and $\bar{\epsilon}$ the effective permittivity.
For bar 3

$$\bar{k}^2=\frac{\pi f_r}{2 f_a}\cot\left(\frac{\pi f_r}{2 f_a}\right)$$

$$\bar{S}=\frac{1}{4\rho l^2 f_a^2(1-\bar{k}^2)}$$

$$\bar{d}=\bar{k}(\bar{S}\bar{\epsilon})^{1/2}.$$

For plates 4 and 5

$$\bar{k}^2 = \frac{\pi}{2}\frac{f_r}{f_a}\cot\left(\frac{\pi}{2}\frac{f_r}{f_a}\right)$$

$$\bar{c} = 4\rho t^2 f_a^2$$

where t is the thickness.
For plate 8

$$\bar{c} = 4\rho t^2 f_r^2.$$

The expressions in the second column in table 1 were then used to calculate the tensor components of d and S. The signs of d_{31} and d_{32} were determined from direct measurement of the charge produced by application of known mechanical stress, while the signs of d_{15} and d_{24} were determined by a trial-and-error procedure. Stiffness coefficients and piezoelectric stress coefficients were calculated using the matrix relations

$$C^E = (S^E)^{-1}$$

and

$$e = dC^E.$$

Relative permittivity coefficients were obtained from capacitance measurements at 1 kHz on X-, Y- and Z-cut plates using a General Radio 1615-A transformer bridge. Thermal expansion coefficients were measured over the temperature range 20–300 °C with a Linseis L76 dilatometer, using bars with lengths parallel to the X, Y and Z directions. The pyroelectric coefficient was measured for the pure material only, by raising the temperature of a Z-cut plate through about 50 °C and measuring the charge released using a Keithley 602 electrometer.

3. Results

3.1. Crystal quality

The pure lithium germanate boules were pear-shaped with their longitudinal axes in the crystallographic [001] (or Z) direction, and each had two parallel flats whose normals were in the [100] (X) direction. They were colourless and transparent and had no visible flaws. The measured density (3·48 g cm^{-3}) was very close to the value calculated from published x-ray lattice parameter data (3·49 g cm^{-3}). An x-ray topographical examination confirmed that the material was defect free and showed a complete absence of domain structure. Optical microscopy on etched surfaces also failed to reveal any domains.

The addition of magnesium oxide to the melt caused a severe degradation of crystal quality which could be seen visibly as translucent regions and cracks. This occurred at MgO contents above 1 wt %, while subsequent analysis showed that less than 0·5 wt % was present in regions of crystal which retained high optical quality. The limit of addition of silica before crystal quality was visibly degraded was 2 wt %, and even at lower levels x-ray topographical studies showed the structure to have been disturbed. Figure 3 (plate) shows an x-ray diffraction topograph taken in transmission with synchrotron radiation at Daresbury Laboratory. The specimen was cut from a crystal which contained 0·9 wt % of SiO_2. The striated appearance is almost certainly due to a slight misalignment of

adjacent blocks of crystal, an effect that was not observed in the case of pure Li_2GeO_3 crystals.

3.2. Physical properties

Table 2 records the piezoelectric, elastic and dielectric data obtained from the measurements on pure lithium germanate and two doped crystals. The impurity levels in the doped crystals, expressed as atomic fractions, were 0·04 Si and 0·005 Mg respectively. Thermal expansion coefficients α and temperature coefficients of S_{ij} and C_{ij} are included, the latter being defined by relations of the form

$$T_S = \frac{1}{S(20\,^\circ\mathrm{C})}\frac{\mathrm{d}S}{\mathrm{d}T}$$

where T is the temperature.

The results on pure Li_2GeO_3 are in general agreement with other workers' reported data (Hirano and Matsumura 1974, Volnyanski *et al* 1976, Ikeda and Imazu 1976) and are typical for piezoelectric materials, except that the piezoelectric shear activity is low. The thermal expansion properties are strongly anisotropic with a relatively small coefficient in the polar direction. The expansion in all three directions was linear over the range 20–300 °C. All the on-diagonal stiffness and compliance terms show normal temperature behaviour (i.e. T_C negative and T_S positive). Thus the elastic properties of lithium germanate appear to show no anomalous variation with temperature. The main effects of the silicon substitution were an increase in the shear stiffness coefficients C_{44} and C_{55}, a reduction in the piezoelectric activity, and a reduction in magnitude (but not sign) of the temperature coefficient of C_{66}. The magnesium substitution, though it degraded the crystal quality badly, had surprisingly little effect on the elastic and piezoelectric properties. The piezoelectric activity in the polar direction was in fact enhanced, k_{33} and d_{33} being about 15% higher than for the pure crystal. With the above-mentioned exception the temperature coefficients of the elastic moduli were virtually unchanged by either substitution.

3.3. Evaluation of the crystals with regard to surface wave applications

Because the elastic moduli of lithium germanate show no anomalous variation with temperature it is very unlikely that a zero temperature coefficient cut for surface waves exists. Moreover the material appears to offer no advantage with regard to wave velocity. The values of bulk shear wave velocity in table 2 lead to an estimated surface wave velocity of the order of 3500 m s^{-1}, while direct measurement on a *Y*-cut, *Z*-propagating device gave the value 3300 m s^{-1}. These values are little different from those for ST quartz (3160 m s^{-1}) and *YZ* lithium niobate (3490 m s^{-1}). Although moderately high coupling factors were observed with lithium germanate ($k_{33}=0{\cdot}28$ and $k_{32}=0{\cdot}19$ compared with $k_{11}=0{\cdot}10$ for quartz), it does not follow that the coupling to surface waves will be better than for quartz. Doping the crystals with either silicon or magnesium, to as high a level as the structure will tolerate, causes small changes in some of the elastic and piezoelectric coefficients but no significant change in their temperature dependence.

4. Conclusions

The results given above confirm the piezoelectric properties of pure lithium germanate published previously and indicate that it is very unlikely that the material possesses a

Table 2. Properties of Si- and Mg-doped Li_2GeO_3 and pure Li_2GeO_3 (Si concentration 4·0 at %, Mg concentration 0·5 at %).

Property	Substituent element			Standard deviation	Property	Substituent element			Standard deviation
	None	Si	Mg			None	Si	Mg	
S_{11}^E (10^{-12} m^2 N^{-1})	9·43	9·41	9·54	0·01	C_{11}^E (10^{10} N m^{-2})	11·2	11·1		0·2
S_{12}^E	−1·10	−1·82		0·08	C_{12}^E	1·6	2·0		0·15
S_{13}^E	−1·73	−0·91		0·07	C_{13}^E	2·35	1·25		0·15
S_{22}^E	10·42	10·42	10·50	0·01	C_{22}^E	10·1	10·0		0·2
S_{23}^E	−1·79	−0·81		0·05	C_{23}^E	2·2	1·1		0·1
S_{33}^E	9·46	9·42	9·62	0·01	C_{33}^E	11·4	10·8		0·2
S_{44}^E	16·8	14·4	16·4	0·1	C_{44}^E	5·96	6·96	6·10	0·02
S_{55}^E	20·6	18·9	21·6	0·1	C_{55}^E	4·85	5·28	4·63	0·02
S_{66}^E	24·8	28·1		0·3	C_{66}^E	4·04	3·56		0·05
Ts_{11} (10^{-6} K^{-1})	110	115	120	2	Tc_{11} (10^{-6} K^{-1})	−35	−160		30
Ts_{22}	180	170	170	3	Tc_{22}	−110	−205		30
Ts_{33}	280	270	280	20	Tc_{33}	−230	−275		30
Ts_{44}	80	105	130	2	Tc_{44}	−80	−105	−130	2
Ts_{55}	120	110	170	4	Tc_{55}	−120	−110	−170	4
Ts_{66}	270	160		10	Tc_{66}	−270	−160		10
d_{15} (10^{-12} C N^{-1})	−8·5	1·4		0·1	e_{15} (C m^{-2})	−0·41	0·074		
d_{24}	−7·0	−5·0		0·1	e_{24}	−0·42	−0·35		
d_{31}	−4·1	−2·6	−3·5	0·05	e_{31}	−0·36	−0·31		
d_{32}	−5·8	−5·3	−5·1	0·05	e_{32}	−0·47	−0·51		
d_{33}	8·2	7·0	9·5	0·1	e_{33}	0·71	0·67		
k_{15}	0·09	0·08	0·09	0·01	α_{11} (10^{-6} K^{-1})	18	18·5	18	0·2
k_{24}	0·085	0·07	0·08	0·005	α_{22}	21	21·5	21·5	0·2
k_{31}	0·12	0·09	0·12	0·01	α_{33}	5·5	5·5	5·5	0·5
k_{32}	0·19	0·17	0·17	0·005					
k_{33}	0·28	0·24	0·33	0·005	Density (g cm^{-3})	3·48	3·45	3·46	0·01
$\frac{1}{\epsilon_0}\epsilon_{11}^\tau$	6·3	6·6	6·4	0·1	Pyroelectric coefficient (10^{-4}C m^{-2} K^{-1})	0·23			
ϵ_{22}^τ	6·5	6·8	6·6	0·1					
ϵ_{33}^τ	10·1	10·1	9·7	0·1					

Acoustic wave velocities (pure Li_2GeO_3, 20°C)

Bulk waves, longitudinal modes	Bulk waves, shear modes	Surface waves
X-propagating 5·7 × 10^3 m s^{-1}	'44' mode 4·1 × 10^3 m s^{-1}	*Y*-cut, *Z*-propagating
Y-propagating 5·4 × 10^3 m s^{-1}	'55' mode 3·7 × 10^3 m s^{-1}	3·3 × 10^3 m s^{-1}
Z-propagating 5·7 × 10^3 m s^{-1}	'66' mode 3·4 × 10^3 m s^{-1}	

zero temperature coefficient of delay. They also show that the crystals do not readily accept foreign ions such as Si and Mg and that the overall effect of foreign ions is to uniformly degrade the piezoelectric characteristics.

Acknowledgments

A M Glazer wishes to thank the Director and staff of the Daresbury Laboratory for access to the NINA synchrotron radiation facility, and the Wolfson Foundation for providing funds. C O'Hara is grateful to R W Whatmore and J W Burgess for helpful discussions. The work was carried out with the support of the Procurement Executive, Ministry of Defence, sponsored by DCVD.

References

Ainger F W, Rich G J, Robertson D S, Saunders A F and Young A S 1971 *Electron. Lett.* **7** 13–4
Dridenbaugh P M, Carruthers J R, Dziedzic J M and Nash F R 1970 *Appl. Phys. Lett.* **17** 104–6
Hirano H and Matsumura S 1974 *Japan. J. Appl. Phys.* **13** (1) 17–23
Ikeda T and Imazu I 1976 *Japan. J. Appl. Phys.* **15** 1451–54
IRE Standards 1958 *Proc. IRE* **46** 764–78
Lock P J 1971 *Appl. Phys. Lett.* **19** 390–1
Namamatsu S, Doi K and Takahashi M 1973 *NEC Research and Development, Japan*, no. 28 pp 72–9
Vollenkle H and Wittmann A 1968 *Monatshafte Chem.* **99** 244–50
Volnyanski M D, Grzhegorzhevski O A, Kudzin A Yu and Flerova S A 1976 *Sov. Phys.—Solid St.* **18** 497
Watton R, Smith C and Jones G R 1976 *Ferroelectrics* **14** 719–21

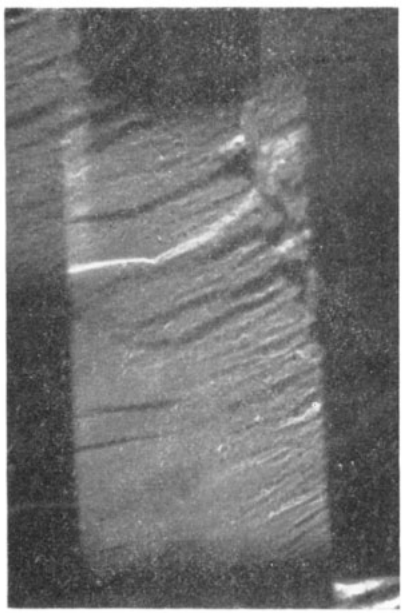

Figure 3. X-ray diffraction topograph of a silicon-doped Li_2GeO_3 crystal (0·9 wt % SiO_2). (Magnification ×40, reduced by ×50% in printing.)